CHAPTER 95

LINEAR AND NONLINEAR WAVE FORCES EXERTED ON A SUBMERGED HORIZONTAL PLATE

Haruyuki Kojima [1], Akinori Yoshida [2] and Tetuya Nakamura [3]

ABSTRACT

Linear and Nonlinear wave forces exerted on a submerged horizontal plate are studied using the method of matched eigenfunction expansions for velocity potential together with the perturbation technique up to second order. Energy damping coefficients are introduced in the formulation to incorporate the effects of vortices and wave breaking. The theoretical results are compared with experimental data to obtain validity and limits of the second-order solution. The theory with proper energy damping coefficients can well simulate the wave forces even when wave breaking occurs over the plate. The second-order oscillatory wave force is relatively small as compared to the first-order one, while time-independent, steady wave force becomes comparable with the first-order one at small relative water depth and its direction is always upward.

1 INTRODUCTION

Wave interactions with a submerged horizontal plate have been extensively studied both theoretically and experimentally. Most of the studies, however, deal with linear wave interactions, namely, reflection and transmission characteristics of waves from the submerged plate (e.g., Ijima *et al.*, 1970, and Patarapanich *et al.*, 1989). These studies concluded that the submerged horizontal plate might be one of the promising wave attenuation devices. There is however little information available on the characteristics of wave forces exerted on the plate except for a work by Patarapanich (1984), especially of nonlinear wave forces. Since wave motion over the plate placed at small submergence depth is highly nonlinear, higher harmonic generation usually occurs; the second harmonic wave increases

[1]Dept. of Civil Engineering, Kyushu Kyouritu Univ., 1-8 Jiyuugaoka, Yahatanishi-ku, Kitakyushu, 807, Japan
[2]Dept. of Civil Engineering Hydraulics, Kyushu Univ., Fukuoka, Japan
[3]Nihonkokudokaihatu Company, Tokyo, Japan

significantly over the plate and at the end of the plate the second harmonic sometimes becomes greater than the first one (Kojima *et at.*, 1990). It is of great interest to study the contribution of the higher harmonic forces to the total wave force. The information on these forces and the overturning moment is essential in designing such a structure.

The main objective of this study is to present a theoretical solution of linear and nonlinear wave forces exerted on a submerged horizontal plate and to understand their characteristics. The solution obtained is valid to second order. Numerical results are compared with experimental data to show the validity and limitation of the second-order solution. The characteristics of wave forces under the extreme condition such as breaking waves are also examined. The study is restricted to the two-dimensional cases of regular waves approaching normal to the thin plate fixed at various submergence below the water surface.

2 THEORETICAL FORMULATION

2.1 Governing Equations

The nonlinear interaction problem is treated as the water wave boundary value problem for the second-order velocity potential since potential flow assumptions may be valid. Let us consider the second-order Stokes' wave, with its first-order amplitude ζ_0, wave number k, and angular frequency σ, incident upon a submerged horizontal plate from the positive x direction, as shown in Fig. 1. Since the fluid motion may be assumed to be irrotational, incompressible and inviscid, the governing equations for this problem are as follows:
Laplace equation,

$$\frac{\partial^2 \Phi}{\partial x^2} + \frac{\partial^2 \Phi}{\partial z^2} = 0 \tag{1}$$

the kinematic free surface boundary condition,

$$\frac{\partial \zeta}{\partial t} + \frac{\partial \Phi}{\partial x}\frac{\partial \zeta}{\partial x} - \frac{\partial \Phi}{\partial z} = 0 \qquad on \quad z = \zeta(x,t) \tag{2}$$

the dynamic free surface boundary condition with the Bernoulli constant Q,

$$\frac{\partial \Phi}{\partial t} + g\zeta + \frac{1}{2}\left\{\left(\frac{\partial \Phi}{\partial x}\right)^2 + \left(\frac{\partial \Phi}{\partial z}\right)^2\right\} = Q \qquad on \quad z = \zeta(x,t) \tag{3}$$

and the kinematic no-flux condition on the plate surface and sea bottom,

$$\frac{\partial \Phi}{\partial z} = 0 \qquad on \quad z = -h_2, -h_d, -h \tag{4}$$

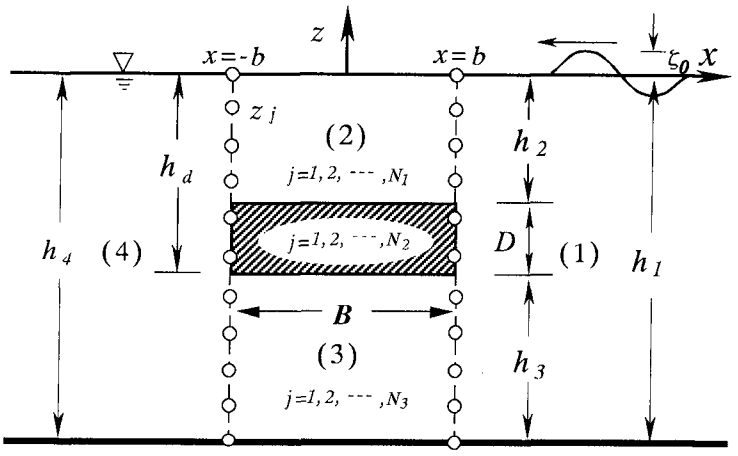

Figure 1 Fluid regions and definition sketch.

2.2 Solutions of first and second order

To obtain solutions for the first- and second-order velocity potential, the velocity potential, water elevation and Bernoulli constant are expanded by the perturbation approach in terms of power series in a small parameter ϵ ($= k\zeta_0$) and the combined free surface boundary condition is applied on the still mean water level with help of the Taylor expansion. Then, the velocity potential $\Phi(x, z, t)$ can be given by

$$\Phi(x,z,t) = \frac{g}{k\sigma} Re\Big[\epsilon\phi_1^{(1)}(x,z)\exp(i\sigma t) + \epsilon^2\{\phi_0^{(2)}(x,z) + \phi_2^{(2)}(x,z)\exp(i2\sigma t)\} + \cdots\Big] \tag{5}$$

in which $\phi_1^{(1)}(x,z)$, $\phi_0^{(2)}(x,z)$, $\phi_2^{(2)}(x,z)$ are nondimensional complex functions (hereafter referred to as a potential function) and the subscripts 0, 1 and 2 indicate the degree of harmonic components and the indices (1) and (2) denote the first- and second-order solutions, respectively.

The potential functions $\phi_1^{(1)}$, $\phi_2^{(2)}$, $\phi_0^{(2)}$ in the regions (1), (2) and (4) with the free water surface can be expressed in terms of a power series as

$$\phi_{i1}^{(1)}(x,z) = \sum_{n=0}^{\infty}\{C_{in}\exp(k_{in}x) + D_{in}\exp(-k_{in}x)\}Z(k_{in}z) \tag{6}$$

$$\begin{aligned}\phi_{i2}^{(2)}(x,z) &= \sum_{n=0}^{\infty}\left\{C_{in}^{(2)}\exp(k_{in}^{(2)}x) + D_{in}^{(2)}\exp(-k_{in}^{(2)}x)\right\}Z(k_{in}^{(2)}z) \\ &\quad + \sum_{m=0}^{\infty}\sum_{p=0}^{\infty}\Pi_{mp}(x,z)\end{aligned} \tag{7}$$

$$\begin{aligned}\phi_0^{(2)}(x,z) &= \overline{C_0^{(2)}}\frac{x}{b} + \overline{D_0^{(2)}} \\ &+ \sum_{n=1}^{\infty}\left\{\overline{C_n^{(2)}}\exp\left(\frac{n\pi}{h}x\right) + \overline{D_n^{(2)}}\exp\left(-\frac{n\pi}{h}x\right)\right\}\cos\frac{n\pi}{h}z \\ &+ \sum_{m=0}^{\infty}\sum_{p=0}^{\infty}\Pi_{mp}^{*}(x,z) \end{aligned} \tag{8}$$

where $C_{in}^{(q)}$, $D_{in}^{(q)}$, $\overline{C_{in}^{(q)}}$, $\overline{D_{in}^{(q)}}$ indicate unknown coefficients of $O(\epsilon^q)$, the subscript i denotes the corresponding fluid regions, and the eigenfunction $Z(k_{in}^{(q)}z)$ is written by

$$Z(k_{in}^{(q)}z) = \frac{\cos k_{in}^{(q)}(z+h_i)}{\cos k_{in}^{(q)}h_i} \tag{9}$$

The eigenvalues $k_{in}^{(q)}$ can be found from the following dispersion relationship.

$$\frac{(q\sigma)^2 h_i}{g} = -k_{in}^{(q)}h_i\tan k_{in}^{(q)}h_i \qquad (i=1,2,4 \quad q=1,2) \tag{10}$$

When $n=0$, it becomes an imaginary number ($k_{i0}^{(q)} = ik_i^{(q)}$) and a real number when $n \neq 0$. $\Pi_{mp}(x,z)$ and $\Pi_{mp}^{*}(x,z)$ in Eqs. (7) and (8) are given by

$$\left.\begin{aligned}\Pi_{mp}(x,z) &= \frac{\lambda(k_m,k_p)}{\mu_1(k_{mp})}Q_{mp}(x)Z(k_{mp}z) + \frac{\overline{\lambda}(k_m,k_p)}{\mu_1(\overline{k_{mp}})}\overline{Q}_{mp}(x)Z(\overline{k_{mp}}z) \\ \Pi_{mp}^{*}(x,z) &= \frac{\Upsilon(k_p)}{\mu_2(k_{mp}^{*})}Q_{mp}^{*}(x)Z(k_{mp}^{*}z) + \frac{\Upsilon(k_p)}{\mu_2(\overline{k_{mp}^{*}})}\overline{Q_{mp}^{*}}(x)Z(\overline{k_{mp}^{*}}z)\end{aligned}\right\} \tag{11}$$

where

$$\left.\begin{aligned}Q_{mp}(x) &= C_mC_p\exp(k_{mp}x) + D_mD_p\exp(-k_{mp}x) \\ \overline{Q}_{mp}(x) &= C_mD_p\exp(\overline{k_{mp}}x) + C_pD_m\exp(-\overline{k_{mp}}x) \\ Q_{mp}^{*}(x) &= C_mC_p^{*}\exp(k_{mp}^{*}x) + D_mD_p^{*}\exp(-k_{mp}^{*}x) \\ \overline{Q}_{mp}^{*}(x) &= C_mD_p^{*}\exp(\overline{k_{mp}^{*}}x) + C_p^{*}D_m\exp(-\overline{k_{mp}^{*}}x)\end{aligned}\right\} \tag{12}$$

$$\left.\begin{aligned}\lambda(k_m,k_p) &= \frac{i}{2k}\left(3\Gamma^2 + 2k_mk_p + k_p^2\right), \quad \Upsilon(k_p) = \frac{i}{2k}\left(\Gamma^2 + k_p^2\right) \\ \overline{\lambda}(k_m,k_p) &= \frac{i}{2k}\left(3\Gamma^2 - 2k_mk_p + k_p^2\right)\end{aligned}\right\} \tag{13}$$

$$\left.\begin{aligned}\mu_1(k_{mp}) &= 4\Gamma + k_{mp}\tan k_{mp}h, \quad \mu_2(k_{mp}^{*}) = k_{mp}^{*}\tan(k_{mp}^{*}h) \\ \mu_1(\overline{k_{mp}}) &= 4\Gamma + \overline{k_{mp}}\tan\overline{k_{mp}}h, \quad \mu_2(\overline{k_{mp}^{*}}) = \overline{k_{mp}^{*}}\tan(\overline{k_{mp}^{*}}h)\end{aligned}\right\} \tag{14}$$

$$\left.\begin{aligned} k_{mp} &= k_m + k_p\ , \quad \overline{k_{mp}} = k_m - k_p\ , \quad \Gamma = \sigma^2/g \\ k^*_{mp} &= k_m + k^*_p\ , \quad \overline{k^*_{mp}} = k_m - k^*_p \end{aligned}\right\} \tag{15}$$

The index * designates the complex conjugate of the variables. Note that $\phi_0^{(2)}(x,z)$, given by Eq.(8) and representing the steady component of the second-order potential function, contributes to neither the second-order water surface displacement nor wave pressure exerted on the plate. The interpretation of the solution for $\phi_2^{(2)}(x,z)$ is discussed elsewhere (Kojim *et al.*, 1994).

The first- and second-order solutions for the fluid region beneath the plate are assumed to have the following form:

$$\begin{aligned} \phi_3^{(q)}(x,z) &= C_{30}^{(q)}\frac{x}{b} + D_{30}^{(q)} \\ &+ \sum_{n=1}^{\infty}\left\{C_{3n}^{(q)}\exp\left(\nu_n x\right) + D_{3n}^{(q)}\exp\left(-\nu_n x\right)\right\}\cos\nu_n(z+d) \end{aligned} \tag{16}$$

in which $\nu_n = n\pi/h_3$ and $q = 1, 2$.

The unknown coefficients in the first- and second-order solutions should be determined by satisfying the no-flux conditions along the vertical faces of the plate as well as flow continuity conditions over the vertical planes separating the fluid regions. Instead of using a conventional technique employing the orthogonality of the eigenfunctions (Ijima,1971, and Massel, 1983), a "collocation" method of matching is applied in determining unknown coefficients in the expansions. A detailed explanation of the procedure is presented by Kojima *et al.* (1994) and Yoshida *et al.* (1990).

2.3 Linear and Nonlinear Wave Forces

2.3.1 Expressions for dynamic wave pressures

The dynamic pressure due to wave action against a submerged horizontal plate can be obtained from the unsteady Bernoulli equation. Like the velocity potential $\Phi(x,z,t)$, the dynamic pressure $p(x,z,t)$ may be expanded in terms of power series in ϵ, and substituting the determined velocity potential into the Bernoulli equation and collecting terms of each order in ϵ yield the non-dimensional dynamic pressure $p(x,z,t)$ to second order in the following form.

$$\begin{aligned} \frac{p(x,z,t)}{\rho g\zeta_0} &= p^{(1)}(x,z,t) + \epsilon p^{(2)}(x,z,t) \\ &= Re\left[p_1^{(1)}(x,z)\exp(i\sigma t) + \epsilon\left\{p_0^{(2)}(x,z) + p_2^{(2)}(x,z)\exp(i2\sigma t)\right\}\right] \end{aligned} \tag{17}$$

where

$$p_1^{(1)}(x,z) = -i\phi_1^{(1)} \tag{18}$$

$$p_0^{(2)}(x,z) = -\frac{g}{4k\sigma^2}\left\{\frac{\partial\phi_1^{(1)}}{\partial x}\frac{\partial\phi_1^{(1)*}}{\partial x} + \frac{\partial\phi_1^{(1)}}{\partial z}\frac{\partial\phi_1^{(1)*}}{\partial z}\right\} + Q^{(2)} \tag{19}$$

$$p_2^{(2)}(x,z) = -2i\phi_2^{(2)} - \frac{g}{4k\sigma^2}\left\{\left(\frac{\partial\phi_1^{(1)}}{\partial x}\right)^2 + \left(\frac{\partial\phi_1^{(1)}}{\partial z}\right)^2\right\} \tag{20}$$

In the above equations $p_1^{(1)}(x,z), p_0^{(2)}(x,z), p_2^{(2)}(x,z)$ are non-dimensional dynamic pressure where the superscripts (1) and (2) denote the first- and second-order dynamic pressures, respectively, and $Q^{(2)}$ is the Bernoulli constant.

2.3.2 Vertical wave force

The vertical wave forces exerted on a horizontal plate located at an arbitrary depth z can be obtained by integrating wave pressures in regions (2) and (3) from $-b$ to b in the direction of x

$$F_Z(z,t) = \frac{f_Z(z,t)}{\rho g\zeta_0 B} = \int_{-b}^{b}\{p_3(x,z,t) - p_2(x,z,t)\}dx \tag{21}$$

By using Eq. (18) through Eq. (20), the normalized wave forces $f_Z(z,t)/\rho g\zeta_0 B$ can be expressed as

$$\begin{aligned} F_Z = \frac{f_Z(z,t)}{\rho g\zeta_0 B} &= Re\left[\left\{F_{Z_{31}}^{(1)}(z) - F_{Z_{21}}^{(1)}(z)\right\}\exp(i\sigma t)\right. \\ &\left. + \epsilon\left\{\left(F_{Z_{30}}^{(2)}(z) - F_{Z_{20}}^{(2)}(z)\right) + \left(F_{Z_{32}}^{(2)}(z) - F_{Z_{22}}^{(2)}(z)\right)\exp(i2\sigma t)\right\}\right] \end{aligned} \tag{22}$$

Since the first-order term is well-known, only the second-order ones are given as follows:

$$\begin{aligned} F_{Z20}^{(2)}(z) &= \int_{-b}^{b} p_{20}^{(2)}(x,z)dx = \sum_{m=0}^{\overline{n_2}}\sum_{p=0}^{\overline{n_2}}\left[\alpha(k_m,k_p^*)Z(\overline{k_{2mp}}z)R_{mp}^*\right. \\ &\left. + \overline{\alpha}(k_m,k_p^*)Z(k_{2mp}z)\overline{R_{mp}^*}\right] + Q^{(2)} \end{aligned} \tag{23}$$

$$\begin{aligned} F_{Z_{30}}^{(2)}(z) &= \int_{-b}^{b} p_{30}^{(2)}(x,z)dx \\ &= -\frac{g}{4k\sigma^2}\left[\frac{C_{30}C_{30}^*}{b^2} + \frac{C_{30}}{2b^2}\sum_{m=1}^{n_3}\{A(\nu_m)\}\{C_{3m}^* - D_{3m}^*\}Z(\nu_m z)\right. \\ &\quad + \frac{C_{30}^*}{2b^2}\sum_{n=1}^{n_3}\{A(\nu_n)\}\{C_{3n} - D_{3n}\}Z(\nu_n z) \\ &\quad \left. + \sum_{n=1}^{\overline{n}_3}\sum_{m=1}^{\overline{n}_3}\nu_n\nu_m\left\{\widehat{R}_{nm}^* Z(\overline{\nu_{nm}}z) - \overline{\widehat{R}_{nm}^*}Z(\nu_{nm}z)\right\}\right] + Q^{(2)} \end{aligned} \tag{24}$$

$$F_{Z22}^{(2)}(z) = \int_{-b}^{b} p_{22}^{(2)}(x,z)dx = -2i\sum_{n=0}^{n_2^{(2)}}\frac{A(k_{2n}^{(2)})}{2k_{2n}^{(2)}b}\left\{C_{2n}^{(2)} + D_{2n}^{(2)}\right\}Z(k_{2n}^{(2)}z)$$

$$-2i\sum_{m=0}^{\overline{n_2}}\sum_{p=0}^{\overline{n_2}}\left\{\frac{\lambda(k_m,k_p)}{\mu_1(k_{mp})}R_{mp}Z(k_{2mp}z)+\frac{\overline{\lambda}(k_m,k_p)}{\mu_1(\overline{k_{mp}})}\overline{R_{mp}}Z(\overline{k_{2mp}}z)\right\}$$
$$+\sum_{m=0}^{\overline{n_2}}\sum_{p=0}^{\overline{n_2}}\left\{\alpha(k_m,k_p)R_{mp}Z(\overline{k_{2mp}}z)+\overline{\alpha}(k_m,k_p)\overline{R_{mp}}Z(k_{2mp}z)\right\} \tag{25}$$

$$\begin{aligned}F^{(2)}_{Z_{32}}(z)&=\int_{-b}^{b}p^{(2)}_{32}(x,z)dx\\&=-2i\left[\left\{-C^{(2)}_{30}+D^{(2)}_{30}\right\}+\sum_{n=1}^{n_3}\frac{A(\nu_n)}{2\nu_n b}\left\{C^{(2)}_{3n}+D^{(2)}_{3n}\right\}Z(\nu_n z)\right]\\&-\frac{g}{4k\sigma^2}\left[\frac{1}{b^2}C^2_{30}+\frac{1}{b^2}C_{30}\sum_{n=1}^{n_3}A(\nu_n)\left\{C_{3n}-D_{3n}\right\}Z(\nu_n z)\right.\\&\left.+\sum_{n=1}^{\overline{n}_3}\sum_{m=1}^{\overline{n}_3}\nu_n\nu_m\left\{\widehat{R}_{nm}Z(\overline{\nu_{nm}}z)-\overline{\widehat{R}_{nm}}Z(\nu_{nm}z)\right\}\right]\end{aligned} \tag{26}$$

where

$$R^*_{mp}=\begin{cases}C_{2m}C^*_{2p}+D_{2m}D^*_{2p} & (m=p=0)\\ \dfrac{A(2k^*_{2mp})}{2k^*_{2mp}b}\left\{C_{2m}C^*_{2p}+D_{2m}D^*_{2p}\right\} & \begin{pmatrix}m=p\neq 0\\ m\neq p\end{pmatrix}\end{cases} \tag{27}$$

$$\overline{R^*_{mp}}=\begin{cases}\exp(-2k_{2m}b)\left\{C_{2m}D^*_{2p}+C^*_{2p}D_{2m}\right\} & (m=p\neq 0)\\ \dfrac{B(k_{2p},k_{2m})}{2\overline{k^*_{2mp}}b}\left\{C_{2m}D^*_{2p}+C^*_{2p}D_{2m}\right\} & \begin{pmatrix}m=p=0\\ m\neq p\end{pmatrix}\end{cases} \tag{28}$$

$$\widehat{R}^*_{nm}=\frac{A(\nu_{nm})}{2\nu_{nm}b}\left\{C_{3n}C^*_{3m}+D_{3n}D^*_{3m}\right\} \tag{29}$$

$$\overline{\widehat{R}^*_{nm}}=\begin{cases}\exp(-2\nu_n b)\left\{C_{3n}D^*_{3m}+C^*_{3m}D_{3n}\right\} & (n=m)\\ \dfrac{B(\nu_m,\nu_n)}{2\overline{\nu_{nm}}b}\left\{C_{3n}D^*_{3m}+C^*_{3m}D_{3n}\right\} & (n\neq m)\end{cases} \tag{30}$$

$$R_{mp}=\frac{A(k_{2mp})}{2k_{2mp}b}\left\{C_{2m}C_{2p}+D_{2m}D_{2p}\right\} \tag{31}$$

$$\overline{R_{mp}}=\begin{cases}\exp(-2k_m b)\left\{C_{2m}D_{2p}+C_{2p}D_{2m}\right\} & (m=p)\\ \dfrac{B(k_{2p},k_{2m})}{2\overline{k_{2mp}}b}\left\{C_{2m}D_{2p}+C_{2p}D_{2m}\right\} & (m\neq p)\end{cases} \tag{32}$$

$$\widehat{R}_{nm}=\frac{A(\nu_{nm})}{2\nu_{nm}b}\left\{C_{3n}C_{3m}+D_{3n}D_{3m}\right\} \tag{33}$$

$$\overline{\hat{R}_{nm}} = \begin{cases} \exp(-2\nu_n b)\left\{C_{3n}D_{3m} + C_{3m}D_{3n}\right\} & (n = m) \\ \dfrac{B(\nu_m, \nu_n)}{2\overline{\nu_{nm}}b}\left\{C_{3n}D_{3m} + C_{3m}D_{3n}\right\} & (n \neq m) \end{cases} \tag{34}$$

In the above equations, $A(k_{2mp})$, $B(k_{2p}, k_{2m})$, $Z(k_{2p}^{(2)}z)$, $Z(\nu_n z), \cdots$ can be given for each variable in the following forms.

$$\left.\begin{aligned} A(k_{2mp}) &= 1 - \exp(-2k_{2mp}b) \\ B(k_{2p}, k_{2m}) &= \exp(-2k_{2p}b) - \exp(-2k_{2m}b) \\ Z(k_{2p}^{(2)}z) &= \frac{\cos k_{2p}^{(2)}(z + h_2)}{\cos k_{2p}^{(2)}h} \\ Z(\nu_n z) &= \cos \nu_n(z + h_d) \end{aligned}\right\} \tag{35}$$

2.3.3 Horizontal wave forces

The horizontal wave forces exerted on the horizontal plate can be obtained by integrating over the plate thickness from $-h_d$ to $-h_2$. The wave force coefficient $F_x = f_x(z,t)/\rho g \zeta_0 D$ can be expressed as

$$\begin{aligned} F_X = \frac{f_x(x,t)}{\rho g \zeta_0 D} = R\epsilon\Big[&\left(F_{X_{41}}^{(1)}(x) - F_{X_{11}}^{(1)}(x)\right)\exp(i\sigma t) \\ &+ \epsilon\left\{\left(F_{X_{40}}^{(2)}(x) - F_{X_{10}}^{(2)}(x)\right) + \left(F_{X_{42}}^{(2)}(x) - F_{X_{12}}^{(2)}(x)\right)\exp(i2\sigma t)\right\}\Big] \end{aligned} \tag{36}$$

$F_{X_{i1}}^{(1)}(x)$, $F_{X_{i0}}^{(2)}(x)$, and $F_{X_{i2}}^{(2)}(x)$ can be given by the following equations:

$$F_{Xi1}^{(1)}(x) = -2i\sum_{n=0}^{n_i^{(1)}}\left\{C_{in}^{(1)}\exp(k_{in}^{(1)}x) + D_{in}^{(1)}\exp(-k_{in}^{(1)}x)\right\}Y_n^{(1)} \tag{37}$$

$$F_{Xi0}^{(2)}(x) = \sum_{m=0}^{\overline{n_i}}\sum_{p=0}^{\overline{n_i}}\left\{\alpha(k_m, k_p^*)Q_{imp}^*(x)\overline{Y_{mp}^*} + \overline{\alpha}(k_m, k_p^*)\overline{Q_{imp}^*}(x)Y_{mp}^*\right\} + Q^{(2)} \tag{38}$$

$$\begin{aligned} F_{Xi2}^{(2)}(x) = &-2i\sum_{n=0}^{n_i^{(2)}}\left\{C_{in}^{(2)}\exp(k_{in}^{(2)}x) + D_{in}^{(2)}\exp(-k_{in}^{(2)}x)\right\}Y_n^{(2)} \\ &-2i\sum_{m=0}^{\overline{n_i}}\sum_{p=0}^{\overline{n_i}}\left\{\frac{\lambda(k_m, k_p)}{\mu_1(k_{mp})}Q_{imp}(x)Y_{mp} + \frac{\overline{\lambda}(k_m, k_p)}{\mu_1(\overline{k_{mp}})}\overline{Q_{imp}}(x)\overline{Y_{mp}}\right\} \\ &+\sum_{m=0}^{\overline{n_i}}\sum_{p=0}^{\overline{n_i}}\left\{\alpha(k_m, k_p)Q_{imp}(x)\overline{Y_{mp}} + \overline{\alpha}(k_m, k_p)\overline{Q_{imp}}(x)Y_{mp}\right\} \end{aligned} \tag{39}$$

where

$$Y^*_{mp} = \begin{cases} 1.0 & (m = p = 0) \\ \dfrac{2\cos k^*_{mp}(h_3 + D/2)\sin k^*_{mp}D/2}{k^*_{mp}D\cos k^*_{mp}h} & \begin{pmatrix} m = p \neq 0 \\ m \neq p \end{pmatrix} \end{cases} \tag{40}$$

$$\overline{Y^*_{mp}} = \begin{cases} 1.0 & (m = p \neq 0) \\ \dfrac{2\cos \overline{k^*_{mp}}(h_3 + D/2)\sin \overline{k^*_{mp}}D/2}{\overline{k^*_{mp}}D\cos \overline{k^*_{mp}}h} & \begin{pmatrix} m = p = 0 \\ m \neq p \end{pmatrix} \end{cases} \tag{41}$$

$$Y^{(2)}_n = \frac{2\cos k^{(2)}_n(h_3 + D/2)\sin k^{(2)}_n D/2}{k_n D\cos k^{(2)}_n h} \tag{42}$$

$$Y_{mp} = \frac{2\cos k_{mp}(h_3 + D/2)\sin k_{mp}D/2}{k_{mp}D\cos k_{mp}h} \tag{43}$$

$$\overline{Y_{mp}} = \begin{cases} 1.0 & (m = p) \\ \dfrac{2\cos \overline{k_{mp}}(h_3 + D/2)\sin \overline{k_{mp}}D/2}{\overline{k_{mp}}D\cos \overline{k_{mp}}h} & (m \neq p) \end{cases} \tag{44}$$

The subscript i is 1 and 4, denoting regions (1) and (4). Since the water depths in regions (1) and (4) are same, the wave numbers k_m, k_p are equal in these regions.

2.4 Incorporation of the effects of energy damping

To incorporate the effects of energy losses due to vortices generated at the plate ends and wave breaking over the plate, the energy losses are assumed to be expressed in terms of flow resistance proportional to square of local flow velocity and to local flow acceleration. The pressure continuity condition along the vertical plane at $x = b$ may then be written as

$$\frac{1}{\rho}(p_1 - p_2) = -\frac{1}{2}C_D|v_1|v_1 - C_M\frac{\partial v_1}{\partial t} \tag{45}$$

where C_D and C_M are energy loss coefficients. By using the Lorentz concept, linearizing a nonlinear term with respect to time and expressing the dynamic wave pressure and velocity in the velocity potential yield the following boundary condition for the potential continuity.

$$\phi_1 - \phi_2 = \beta|\frac{\partial\phi_1}{\partial x}|\frac{\partial\phi_1}{\partial x} - C_M\frac{\partial\phi_1}{\partial x} \tag{46}$$

where

$$\beta = i\frac{4}{3\pi}\frac{g}{\sigma^2 h}\frac{\zeta_0}{h}C_D \tag{47}$$

3 Hydraulic Experiments

Two-dimensional hydraulic experiments are performed to measure the vertical and horizontal wave forces as well as the dynamic pressure along the upper and lower surfaces of the plate using pressure transducers. Fig. 2 illustrates the devices used for these measurements. For horizontal wave forces, as shown on the left-hand side of the figure, two pairs of strain gages were mounted on four steel cylinders attached to the horizontal plate. The horizontal forces may then be obtained through a calibrated strain-force relationship. For vertical wave forces, pressure transducers were mounted on both the top and bottom surfaces of the plate, as shown on the right-hand side of the figure. Integrating pressure distributions along the plate yields vertical wave forces exerted on the plate top and bottom surfaces, and adding these forces gives the resultant vertical wave forces. The height and period of incident waves are varied to investigate the effects of wave breaking over the plate on wave forces.

4 RESULTS AND DISCUSSIONS

4.1 The first- and second-order wave pressures and forces

The components induced by the nonlinear interactions of the second-order theory include a time-independent, steady component and second-harmonic component which constitute the second-order wave pressure and force. Fig. 3 shows comparison between the computed and measured pressure amplitude distributions along the top surface (upper figure) and the bottom surface (lower figure) of the plate. The lines indicate the computed results and the marks the measured. When energy damping is not taken into consideration, i.e. $C_D = C_M = 0.0$, an agreement between the computed and measured pressure distributions is poor, especially for the first harmonic pressure component, as shown in the left-hand side of Fig. 3. This may thus be due to the effects of energy losses caused by the generation of vortices at the two ends of the plate. With proper energy loss coefficients, which are 0.8 for C_D and 0.0 for C_M in this case, both 1st- and 2nd-order solutions agree quite well with the experimental results, as seen in the right-hand side of Fig 3. However, the computed 2nd-order steady component somehow deviates from the measured.

The amplitude of the first- and second-order non-dimensional oscillatory wave forces is shown in Fig. 4, where the thin lines indicate the computed results without consideration of energy damping and the thick lines with consideration of energy damping. By comparing the measured wave forces with the computed, an agreement between them is remarkably good when the submergence depth is not so small and the wave height is fairly small. The effects of energy loss indicated by the thick lines affect the normalized vertical force F_z more than the normalized horizontal one F_x. The computed second-order oscillatory forces $F^{(2)}$, indicated by the broken line, are also consistent with the measured, indicated by

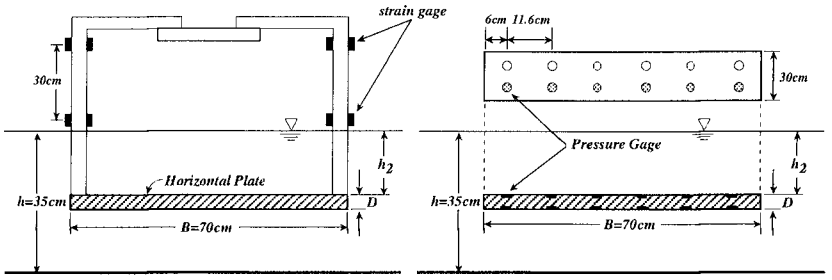

Figure 2 Schematic description of measuring devices for horizontal and vertical wave forces.

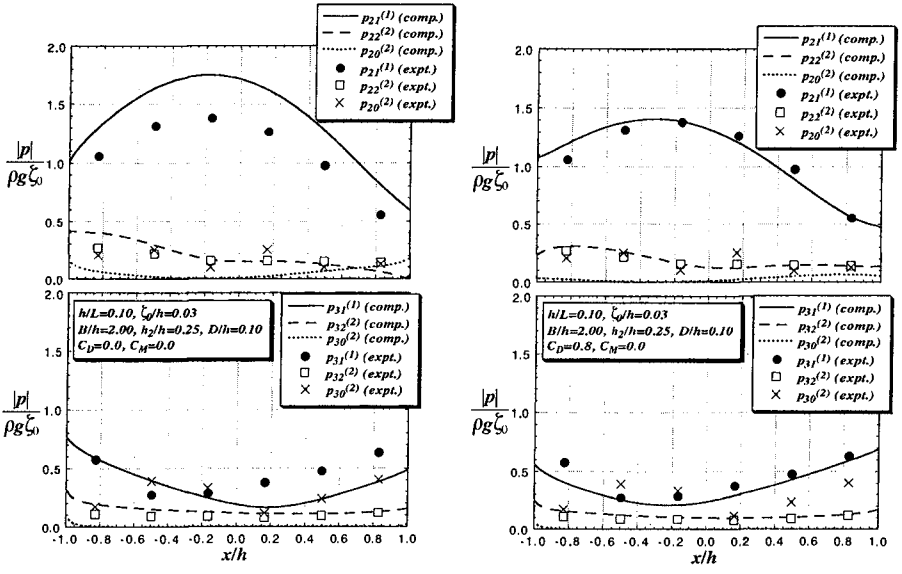

Figure 3 Comparison between computed and experimental wave pressure along the top and bottom surfaces of the plate with and without energy damping consideration.

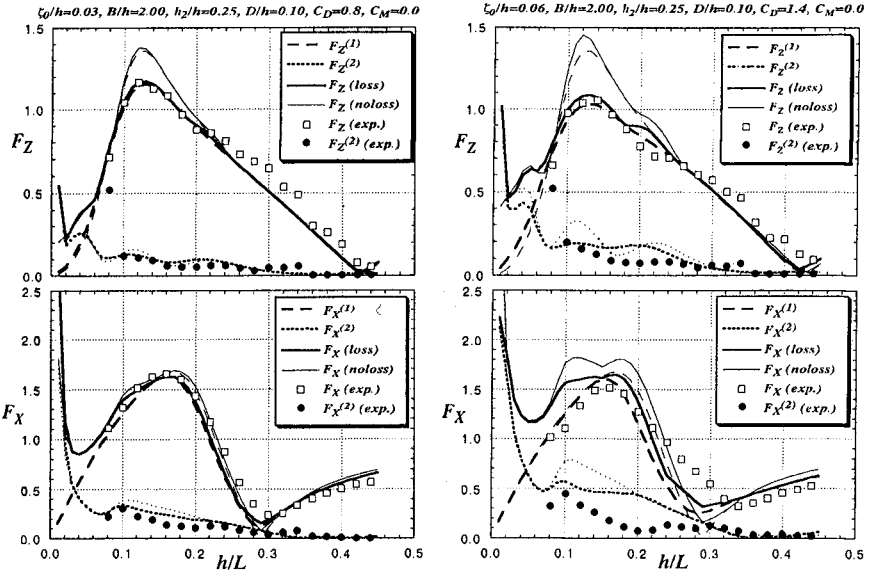

Figure 4 Comparison between computed and measured wave forces exerted on a submerged horizontal plate with $\zeta_0/h = 0.03$ and $\zeta_0/h = 0.06$.

the black circle. Both the vertical and horizontal second-order oscillatory forces are small compared with the first-order ones $F^{(1)}$ and decrease monochromatically with increase in h/L

The right-hand side of Fig. 4 shows the result of a higher incident wave amplitude ($\zeta_0/h = 0.06$), where wave breaking takes place over the plate when the relative water depth is greater than $h/L = 0.14$. The theory with greater C_D value can simulate the total wave forces fairly well even when wave breaking occurs over the plate. Although the theory overpredicts the 2nd-order oscillatory force, the actual values become quite small. Thus the first-order or linear wave forces dominate the total wave forces.

4.2 Variation of wave forces due to the submergence depth

Fig. 5 shows the variations of the normalized 1st-order vertical and horizontal wave forces with relative water depth for three different submergence depths. As the submergence depth h_2/h decreases, the computed results disagree not only quantitatively but also qualitatively with the measured, as depicted in Fig 5. The theory can fairly well predict the value of the maximum vertical and horizontal wave forces up to $h_2/h = 0.15$. At a smaller submergence depth the theoretical values fluctuate with the variation of relative water depth, but the experimental

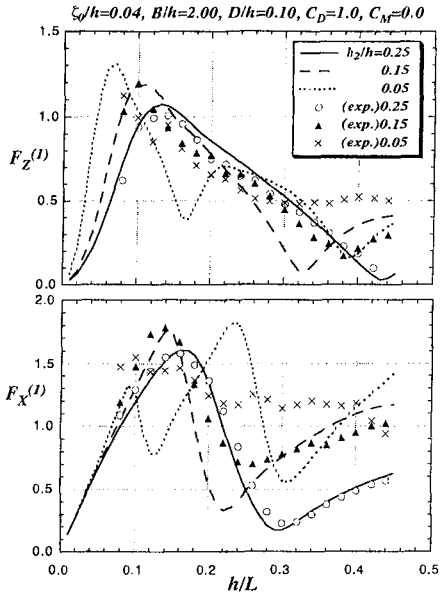

Figure 5 Variations of the first-order wave forces with submergence depth.

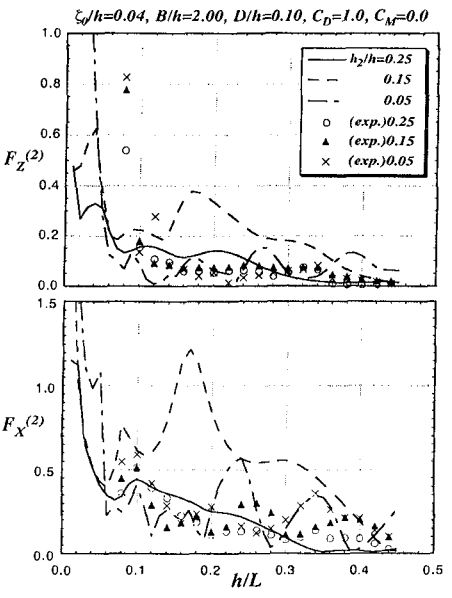

Figure 6 Variations of the second-order wave forces with submergence depth.

ones somewhat flatten over the whole range of relative water depth. The theory also overpredicts the amplitude of the second-harmonic force, as depicted in Fig. 6.

4.3 Variation of time-independent, steady wave forces

Another important wave force for design of a submerged horizontal plate is time-independent, steady force. The variations of normalized vertical steady forces for three different incident waves are delineated in Fig. 7, where a rectangular mark indicates the force exerted on the plate's top surface, a triangular mark on the plate's bottom surface, and a black circle the resultant force. When an incident wave height is relatively small, say $\zeta_0/h = 0.03$, upward steady forces act on the plate's bottom surface, while downward steady forces act on the plate's top. Since the upward forces are almost always greater than the downward forces, the resultant steady forces become uplift ones. The net steady forces exerted on the plate become comparatively large in magnitude at smaller relative water depth, decreasing almost monochromatically with the increase in relative water depth, and at larger relative water depth the forces come closer to zero. As an incident wave height increases, the normalized steady forces exerted on the both top and bottome surfaces become smaller and the direction of the forces exerted on the top surface changes to the upward at smaller relative water depth.

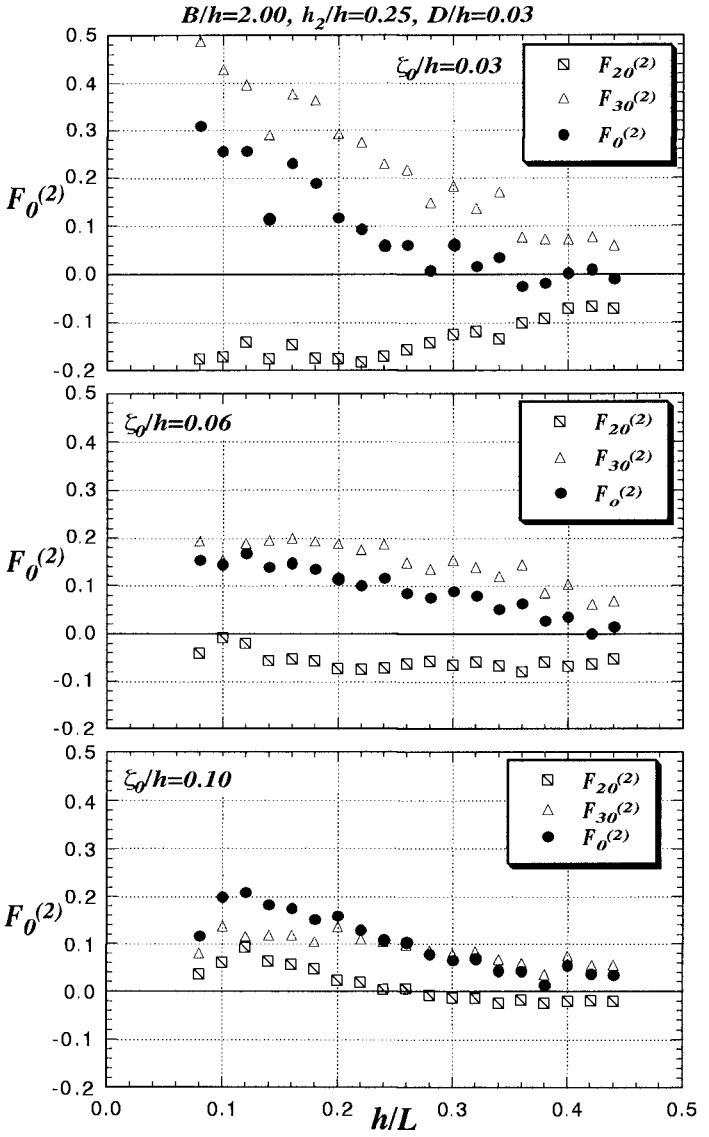

Figure 7 Variations of the steady wave forces with relative water depth for different incident wave heights.

5 CONCLUSIONS

The following conclusions are obtained from this study:

1. Linear and nonlinear dynamic wave pressures and forces exerted on a submerged horizontal plate are explained through the non-transient, finite amplitude wave theory that is valid to second order.
2. The theory with proper energy damping coefficients can well simulate the wave forces even when wave breaking occurs over the plate. The second-order wave forces are relatively small as compared to the first-order ones.
3. For the plate placed close to the water surface, the computed wave forces are qualitatively inconsistent with the measured; the computed first-order oscillatory wave forces fluctuate with relative water depth, while the measured vary almost linearly.
4. When wave height is relatively small, an upward steady force acts on the plate bottom surface, while a downward steady force acts on the plate top surface; the direction of the resultant force depends on their magnitude. The steady net uplift force becomes comparatively large in magnitude at smaller relative water depth, decreasing almost monochromatically with increase in relative water depth.

REFERENCES

Ijima, T. *et al.* (1970): "Analytical study of breakwater and quay with horizontal plate," *Proc. of the 17th Japanese Conf. on Coastal Eng.*, pp. 97-106 (in Japanese).

Ijima, T. (1971): "Solutions of boundary value problems in recent wave theory and their application," *Summer Seminar on Hydr. Eng.*, JSCE, Course B, pp.B.1.1-B.1.30 (in Japanese).

Kojima, H., T. Ijima, and A. Yoshida (1990): "Decomposition and interception of long waves by a submerged horizontal plate," *Proc. 22nd ICCE*, pp.1228-1241.

Kojima, H., A. Yoshida, and T. Ijima (1994): "Second-order interactions between water waves and a submerged horizontal plate," *Coastal Engineering in Japan*, in press.

Massel, S.R. (1983): "Harmonic generation by waves propagating over a submerged step," *Coastal Engineering, Vol. 7*, pp.350-380.

Patarapanich, M. and Hin-Fatt Cheong (1989): "Reflection and transmission characteristics of regular and random waves from a submerged horizontal plate," *Coastal Engineering, Vol. 13*, pp.161-182.

Patarapanich, M. (1984): "Forces and moment on a horizontal plate due to wave scattering," *Coastal Engineering, Vol. 8*, pp.279-301.

Yoshida, A., H. Kojima and Y. Tsurumoto (1990).: "A collocation method of matched eigenfunction expansions on the boundary-value problem of wave-structure interactions," *Proc. JSCE, 417/II-13*, pp.265-274 (in Japanese).